Досліджено режими роботи однофазного активного випрямляча струму у випадку широтно-імпульсної модуляції по прямокутно-ступінчатому закону і навантаження у вигляді тягового двигуна постійного струму. Розглянуто однофазну мостову схему випрямляча з розрядним діодом. Розроблено математичну модель випрямляча і визначено основні розрахункові співвідношення для широтно-імпульсної модуляції при прямокутно-ступінчатій формі модуляційного сигналу. На комп'ютерній моделі досліджено електромагнітні процеси при трьох значеннях частоти модуляції (900, 1200, 1800 Гц). Встановлено особливості впливу глибини і частоти модуляції на коефіцієнт потужності випрямляча і ступінь спотворення синусоїдальності форми кривих напруги та струму в мережі живлення.

Двигун постійного струму на сьогодні залишається основним типом тягового двигуна магістральних електровозів змінного струму напругою 25 кВ, 50 Гц в Україні та в ряді інших країн. Для живлення таких двигунів як правило застосовують випрямлячі на діодах або тиристорах. Разом з тим відомо, що перетворювачі на повністю керованих напівпровідникових приладах забезпечують більш високу енергетичну ефективність.

Проведені дослідження дозволили встановити, при яких значеннях частоти і глибини модуляції забезпечується високий коефіцієнт потужності (більше 0,9) і мінімальні спотворення синусоїдальності форми напруги і струму в мережі живлення. Це дозволяє визначити раціональні підходи до вибору силових схем і алгоритмів управління активними перетворювачами в тяговому електроприводі електровозів. Ефективність підвищення коефіцієнта потужності і зменшення несинусоїдальності напруги та струму полягає, насамперед, в зниженні витрат електроенергії на тягу поїздів.

За сукупністю обраних критеріїв порівняння найбільш прийнятним для реалізації в тяговому електроприводі електровоза є активний випрямляч струму з частотою модуляції 1200 Гц. Забезпечення високих енергетичних характеристик в широкому діапазоні тягових навантажень може бути досягнуто в багатозонній схемі такого перетворювача

Ключові слова: активний випрямляч струму, коефіцієнт потужності, широтно-імпульсна модуляція, математична модель

UDC 621.314.5:629.423
DOI: 10.15587/1729-4061.2018.131150

ANALYSIS OF OPERATING MODES OF SINGLE-PHASE CURRENT-SOURCE RECTIFIER WITH RECTANGULAR-STEPPED PULSE-WIDTH MODULATION

O. Krasnov
Leading Researcher*
E-mail: uzdlines@gmail.com
B. Liubarskyi
Doctor of Technical Sciences, Professor
Department of electrical transport and diesel locomotive**
E-mail: lboris1911@ukr.net
V. Bozhko
PhD, Senior Researcher*
E-mail: bozhkovv81@gmail.com
O. Petrenko
PhD, Associate Professor
Department of electrical transport
O. M. Beketov National University of Urban Economy in Kharkiv
Marshala Bazhanova str., 17, Kharkiv, Ukraine, 61002
O. Dubinina
Doctor of Pedagogical Sciences, PhD, Associate Professor
Department of computer mathematics and data analysis**
E-mail: vovochka88@ukr.net
R. Nuriiev
Postgraduate Student
Department of electrical transport and diesel locomotive**
E-mail: ramkhua@gmail.com
*Department of railway infrastructure and traction
Branch "Design and survey institute of railway transport" of Public Joint-Stock Company "Ukrainian zaliznytsia"
Yevhena Kotliara str., 7, Kharkiv, Ukraine, 61052
**National Technical University "Kharkiv Polytechnic Institute"
Kyrpychova str., 2, Kharkiv, Ukraine, 61002

1. Introduction

When choosing technical solutions for modern high-voltage converters used in the electric drive, it is necessary to seek for ensuring high power efficiency and electromagnetic compatibility with the mains supply [1, 2]. Economic power consumption by electric drives is achieved with optimum control of their operating modes [3]. Active transducers with pulse-width modulation (PWM) have such capabilities [4]. In particular, active current-source rectifiers (ACSR) are used as power sources for autonomous current inverters, as well as for regulating the speed of DC motors [5, 6]. Such

rectifiers can replace diode and thyristor converters used on the 25 kV, 50 Hz AC electric rolling stock for power supply of traction motors and auxiliary machines [7]. Therefore, theoretical studies and practical developments of active current-source rectifiers for railway electric traction systems will be relevant.

2. Literature review and problem statement

As it is fairly noted in [8, 10], the number of works dealing with single-phase active current-source rectifiers is insignificant for today. There are no studies related to the practical application of this class of rectifiers on the electric rolling stock. There are theoretical and pilot studies within the development of a new generation of traction converters for 25 kV, 50 Hz and 15 kV, 16⅔ Hz AC commuter electric trains.

In [9], the control scheme and algorithm for the IGBT four-zone rectifier-inverter converter have been proposed (for the VL80R, 2ES5K electric locomotives). According to the results of pilot studies, the power factor of this converter was 0.95 in the entire load range. However, the converter uses phase control, which does not significantly increase the power factor and reduce the total harmonic current distortion of the electric locomotive.

In [8], the new control strategy for the ACSR based on active suppression of resonant phenomena introduced by the input LC filter and correction of unsinusoidality of the contact line current by direct line voltage measurement has been proposed and investigated. This system provides suppression of low-frequency voltage and current harmonics on the electric locomotive current collector.

In [10], the ACSR with a control system in which PI regulators of the rectified current and phase shift between the current collector voltage and the line current generate a reference signal on the ACSR input current has been considered. The other unit generates a compensation signal for the 3rd, 5th and 7th current harmonics. The sum of these signals is the reference for the PWM unit. The studies have been carried out at a modulation frequency of 2 kHz. The experiments have shown that the proposed control system reduces low-frequency distortion of current and approximates its waveform to sinusoidal, including at a distorted line voltage. The total harmonic current distortion (THDi) was 7.61...158.66 % without compensation and 2.75...16.03 % with compensation.

In [11], the operation of the active current-source rectifier (modulation frequency of 2 kHz) under unfavorable operating conditions of the line (voltage dips, jumps in voltage and load) in the traction mode has been investigated. In this case, the rectifier control strategy, which is based on the phase shift control with the active attenuation of line current harmonics has proved to be effective. The reference signal on the ACSR input current is formed by means of the PI power factor controller.

In [12], electromagnetic processes and the principle of constructing the automatic control system for the traction ACSR with constant PWM frequency have been investigated. In this case, the DC regulation has been carried out by shifting the modulating signal phase to form negative polarity sections in the rectified voltage waveform, as in zone-phase controlled thyristor rectifiers.

In [13], the scheme of "serial input, parallel output" of the active rectifier using PWM and high-frequency transformer has been developed. The control system provides regulation and stabilization of the rectified voltage, as well as active filtering of the input rectifier current.

In [14], ripple elimination with double line frequency by setting a decoupling capacitor and a diode in the ACSR circuit has been proposed. However, this scheme is designed for low loads. The issue of the operability of such a scheme in traction electric drives will require additional research.

In [15], control characteristics of active current-source rectifiers, based on null and bridge circuits, with sinusoidal PWM have been obtained. However, in this case, the rectifier power factor when the load changes has not been evaluated.

Thus, the ACSR can perform the following functions:

– active filter, capable of operating with both inductive and capacitive cos φ;

– rectified voltage or current regulator (depending on the control system structure).

At the same time, the above works have not taken into account that the implementation of various PWM algorithms – trapezoidal, vector, etc., is possible in the ACSR [16]. In addition, it is of interest to compare power characteristics of the ACSR for different values of modulation depth and PWM frequency.

3. The aim and objectives of the study

The aim of the study is to analyze the operating modes of the single-phase active current-source rectifier as a rectified voltage regulator. The case of pulse-width modulation with the rectangular-stepped modulating signal at the ACSR load in the form of the DC traction motor is considered.

To achieve the aim, the following objectives were accomplished:

– to develop a mathematical model of the ACSR and to determine the main ratios for pulse-width modulation with the rectangular-stepped modulating signal;

– to study electromagnetic processes in the PWM active current-source rectifier at a modulation frequency of 900, 1,200 and 1,800 Hz, to evaluate the nature of the changes in its power factor;

– to evaluate the effect of the PWM frequency and modulation index on total harmonic distortion in the mains supply;

– to select the most suitable active current-source rectifier for further implementation in the traction electric drive.

4. Mathematical model of the active current-source rectifier and selection of criteria of its efficiency

We consider the electromagnetic processes in the single-phase active current-source rectifier on the example of the single-phase discharge diode bridge circuit (Fig. 1) in the rectification mode. The ACSR keys $K1$–$K4$ are fully controllable, with unidirectional current conduction. Each key consists of the series-connected IGBT transistor and the diode. Such a converter with minor modification of the power circuit can work in the inverter (regenerative) mode with the transfer of energy to the mains supply.

The AC mains supply in the design scheme (Fig. 1) is represented by equivalent EMF e_s, inductance L_s and resistance r_s. The transformer parameters are: L_1, r_1, L_2, r_2 – total inductance and resistance of the primary and secondary windings of the transformer, respectively; M_{12} – mutual inductance between the primary and secondary windings. Parameters of the ACSR

and rectified current circuit: C – input filter capacity; E_d, L_d, r_d – equivalent EMF, inductance and resistance. The scheme also indicates: u_c – input filter capacitor voltage; i_1, i_2, i_v, i_c, i_d – currents in circuit elements.

For the scheme (Fig. 1), the following system of equations can be written:

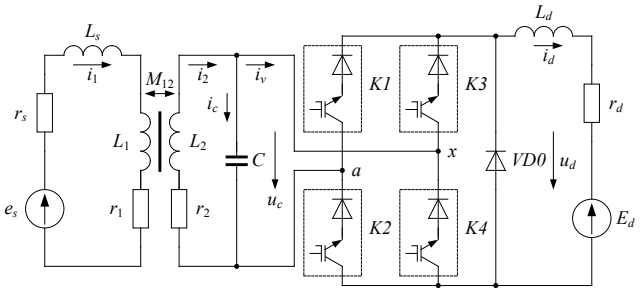

Fig. 1. Design scheme of the single-phase active current-source rectifier

$$\begin{cases} e_s = \sqrt{2}E_s \cdot \sin\omega t, \\ (L_s + L_1)\dfrac{di_1}{dt} + M_{12}\dfrac{di_2}{dt} + (r_s + r_1)i_1 - e_s = 0, \\ L_2\dfrac{di_2}{dt} + M_{12}\dfrac{di_1}{dt} + r_2 i_2 + u_c = 0, \\ -S^* u_c + L_d\dfrac{di_d}{dt} + r_d i_d + E_d = 0, \\ \dfrac{du_c}{dt} = \dfrac{1}{C}i_c, \\ i_v = S^* i_d, \\ i_2 - i_c - i_v = 0. \end{cases} \quad (1)$$

It follows from (1) that the rectified voltage $u_d=S^*u_c$ and the input current i_v depend on the state of the ACSR keys. This state is determined by the unit switching function S^*:

$$S^* = \begin{cases} (s_2^*=1)\wedge(s_3^*=1)\rightarrow 1, \\ (s_1^*=1)\wedge(s_4^*=1)\rightarrow -1, \\ (s_1^*=0)\wedge(s_2^*=0)\wedge(s_3^*=0)\wedge(s_4^*=0)\rightarrow 0, \end{cases} \quad (2)$$

where are the switching functions of the ACSR keys.

The EMF of the DC traction motor [17]:

$$E_d = c_e \Phi n, \quad (3)$$

where c_e is the design constant of the engine; $\Phi=f(I_d)$ is the magnetic flux, Wb; n is the engine speed, rpm.

The average value of the rectified voltage, regulated by the pulse-width modulation method, can be calculated from the formula [18]:

$$U_d = \frac{1}{\pi}\sum_{i=1}^{n}\left[\int_{\alpha_i}^{\beta_i}\sqrt{2}U_2\sin\theta d\theta\right] = \frac{\sqrt{2}U_2}{\pi}\sum_{i=1}^{n}\left[\cos\alpha_i - \cos\beta_i\right], \quad (4)$$

where α_i, β_i are the angles of transition of transistors to the on and off states; n is the number of pulses per half-cycle $T=\pi$; $\theta=\omega t$.

The RMS voltage of the secondary winding of the transformer can be obtained from (4):

$$U_2 = 2{,}22U_d\left[\sum_{i=1}^{n}(\cos\alpha_i - \cos\beta_i)\right]^{-1}. \quad (5)$$

The block diagram of the ACSR control system is shown in Fig. 2, and the PWM pulse-shaping circuits – in Fig. 3. IGBT transistor control pulses are generated at the moments of equality of the stepped modulating signal $\mu\times u_m$ (μ– amplitude modulation index) and the reference sawtooth voltage u_{ref} with the clock modulation frequency f_m. The waveform of the modulating and reference signals (Fig. 3) is assumed to be unipolar. The pulse-height distribution by the control system is carried out by controlling the sign of the sinusoidal signal $u(t)$, synchronized with voltage u_1. As a result, pulse alternating current i_v is formed on the AC terminals a, x, and pulse rectified voltage u_d – in the DC circuit.

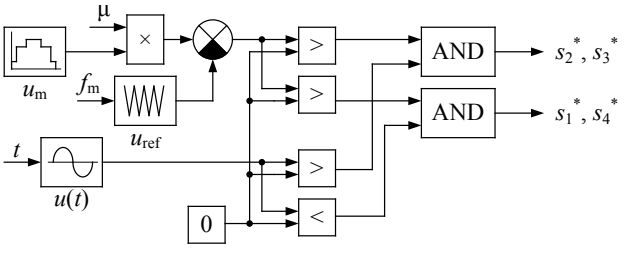

Fig. 2. Block diagram of the ACSR control system

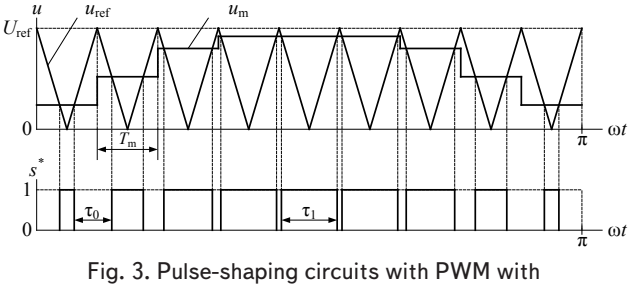

Fig. 3. Pulse-shaping circuits with PWM with the rectangular-stepped modulating signal: U_{ref} – reference voltage amplitude; u_{ref} – reference voltage; u_m –modulating voltage; T_m – pulse-width modulation period; s^* – ACSR switching function; τ_1 – relative pulse duration; τ_0 – relative pause duration; u – voltage; ω – angular line frequency; t – time

The modulating signal is an approximation of a sine wave of the form $f(t)=|\sin\omega t|$ by a step function [16]. In each PWM period, $T_m=1/f_m$, the sine wave segment is replaced by a straight line segment. Such a signal can be characterized by the following parameters [19]: U_m – modulating voltage amplitude; θ_i – phase angle of the ith step $\Delta\theta$ – discrete step of changes in the phase angle; $i=1...n$ – step number; n – number of steps.

In general, there can be any number of steps of the modulating voltage. However, for convenience of the mathematical description of the PWM algorithm, we assume that the number of steps is equal to the number of modulation periods. Then for $\omega t=0...\pi$ we have:

$$n = \frac{f_m}{2f}, \quad (6)$$

$$\Delta\theta = 180^\circ / n, \quad (7)$$

where f is the line frequency, Hz; f_m is the modulation frequency, Hz.

Let us write formulas for determining the ith value of the angle θ and the modulating voltage $u_m(\theta)$:

$$\theta_i = i \cdot \Delta\theta; \quad (8)$$

$$u_m(\theta) = \begin{cases} (0 \le \theta \le \pi/2) \to \mu U_m \cdot \sin\theta, \\ (\pi/2 < \theta \le \pi) \to \mu U_m \cdot \sin(\theta - \Delta\theta). \end{cases} \quad (9)$$

As can be seen from Fig. 3, the value of the modulating signal on the PWM period is proportional to the relative pulse duration on the same period. Let us denote this value by τ_1, and the relative pause duration τ_0. If we assume U_m=1, then τ_1 and τ_0 can be determined by the formulas:

$$\tau_1 = \begin{cases} (0 \le \theta \le \pi/2) \to \mu \cdot \sin\theta, \\ (\pi/2 < \theta \le \pi) \to \mu \cdot \sin(\theta - \Delta\theta); \end{cases} \quad (10)$$

$$\tau_0 = 1 - \tau_1. \quad (11)$$

Thus, in the PWM under consideration, the ACSR control pulses are formed according to the principle similar to the vector PWM of three-phase active converters [20]. As an example, Table 1 presents the results of the calculation of PWM parameters at f_m=900 Hz, μ=1.

Table 1

Results of calculation of PWM parameters (f_m=900 Hz, μ=1)

i	1	2	3	4	5	6	7	8	9
θ_i	20°	40°	60°	80°	100°	120°	140°	160°	180°
τ_1	0.342	0.643	0.866	0.985	0.985	0.985	0.866	0.643	0.342
τ_0	0.658	0.357	0.134	0.015	0.015	0.015	0.134	0.357	0.658

At the repetition period T=π, the modulating voltage can be represented as the following sequence of steps:

$$u_m(\theta) = \begin{cases} (0 \le \theta \le \theta_1) \to \tau_1(\theta_1), \\ (\theta_1 \le \theta \le \theta_2) \to \tau_1(\theta_2), \\ \ldots \\ (\theta_{i-1} \le \theta \le \theta_i) \to \tau_1(\theta_i). \end{cases} \quad (12)$$

The reference signal of a unipolar sawtooth waveform:

$$u_{ref}(t) = \frac{U_{ref}}{\pi} \left| \arcsin\left[\sin\left(\frac{\omega_m}{2} t + \frac{\pi}{2} \right) \right] \right|, \quad (13)$$

where $\omega_m = 2\pi f_m$ is the angular modulation frequency, rad/s.

Switching functions $s_1^* - s_4^*$ of ACSR keys:

$$s_2^* = s_3^* = \begin{cases} (u_2 > 0) \wedge (u_m - u_{ref} > 0) \to 1, \\ (u_2 > 0) \wedge (u_m - u_{ref} \le 0) \to 0; \end{cases} \quad (14)$$

$$s_1^* = s_4^* = \begin{cases} (u_2 < 0) \wedge (u_m - u_{ref} > 0) \to 1, \\ (u_2 < 0) \wedge (u_m - u_{ref} \le 0) \to 0. \end{cases} \quad (15)$$

Regulation of the ACSR rectified voltage is carried out by changing the modulation index μ. According to the formula (4) for f_m=900 Hz, n=9 the average value of the rectified voltage:

$$U_d = \frac{\sqrt{2}\mu U_2}{\pi} \left[(\cos\alpha_1 - \cos\beta_1) + \ldots + (\cos\alpha_9 - \cos\beta_9) \right]. \quad (16)$$

Taking into account the symmetry of the rectified voltage waveform:

$$U_d = \frac{\sqrt{2}\mu U_2}{\pi} \times \\ \times \left[2(\cos\alpha_1 - \cos\beta_1 + .. + \cos\alpha_3 - \cos\beta_3) + \right. \\ \left. + 3(\cos\alpha_4 - \cos\beta_4) \right]. \quad (17)$$

Similarly, for f_m=1,200 Hz, n=12:

$$U_d = \frac{\sqrt{2}\mu U_2}{\pi} \left[2(\cos\alpha_1 - \cos\beta_1 + \ldots + \cos\alpha_6 - \cos\beta_6) \right]. \quad (18)$$

Equations (1)–(3), (6), (7), (10)–(15) are a mathematical model of the active current-source rectifier. To solve them, the MATLAB model, shown in Fig. 4 is developed. Elements of the power part of the ACSR model are units of the traction transformer *TT*, input filter *Cf*, active current-source rectifier ACSR and EMF of the traction motor *Ed* (Fig. 4, *a*). The control system model consists of shaping units of the modulating voltage *U_mod*, reference voltage *U_op*, sinusoidal signal *U_sinhr*, synchronized with voltage u_1, comparison operators «>», «<» and logical elements AND. The input signals of the control system are the PWM frequency *F_mod* and the modulation index *M*, and the output signals are IGBT pulse control signals *S01*, *S02*.

In the research, the following parameters of the model were adopted: the traction substation with the 40 MV·A transformer, line section of 10 km, the power of the traction transformer of 4.35 MV·A, powered by the ACSR of a single traction engine DTK-820 of electric locomotives 2EL5. Parameters of the mains supply: E_s=25,000 V; L_s=0.022922 H; r_s=1.7597 ohms. Transformer parameters: L_1=57.278573 H; r_1=0.314 ohms; U_2=1260 V; L_2=0.145497 H; r_2=0.00351 ohms; M_{12}=2.882512 H. Parameters of the rectified current circuit: L_d=0.00957 H; r_d=0.084174 ohms. Electromagnetic processes in the ACSR were investigated for three values of modulation frequency – 900 Hz, 1,200 Hz and 1,800 Hz. The modulation index varied within μ=0.2...1.

As the ACSR efficiency criteria, determined in virtual experiments, the following indicators were selected:

– average rectified voltage (U_d, V);

– power factor, measured at the terminals of the primary winding of the transformer (K_p);

– total harmonic voltage distortion u_1 (K_U, %);

– total harmonic current distortion i_1 (K_I, %).

The power factor K_p was calculated by the formula:

$$K_p = \left(\int_0^T u_1 i_1 dt \right) / \sqrt{\left(\int_0^T u_1^2 dt \right) \left(\int_0^T i_1^2 dt \right)}. \quad (19)$$

The average power factor K_{ap} in the entire range of regulation:

$$K_{ap} = \left(\sum_{j=1}^{m} K_{pj} \right) / m, \quad (20)$$

where j=1...m is the number of the experiment; m is the number of measurements.

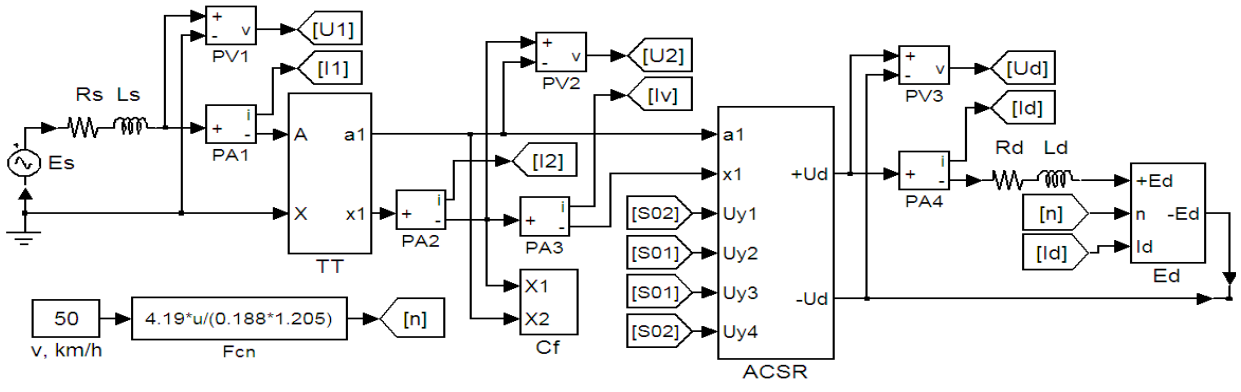

a

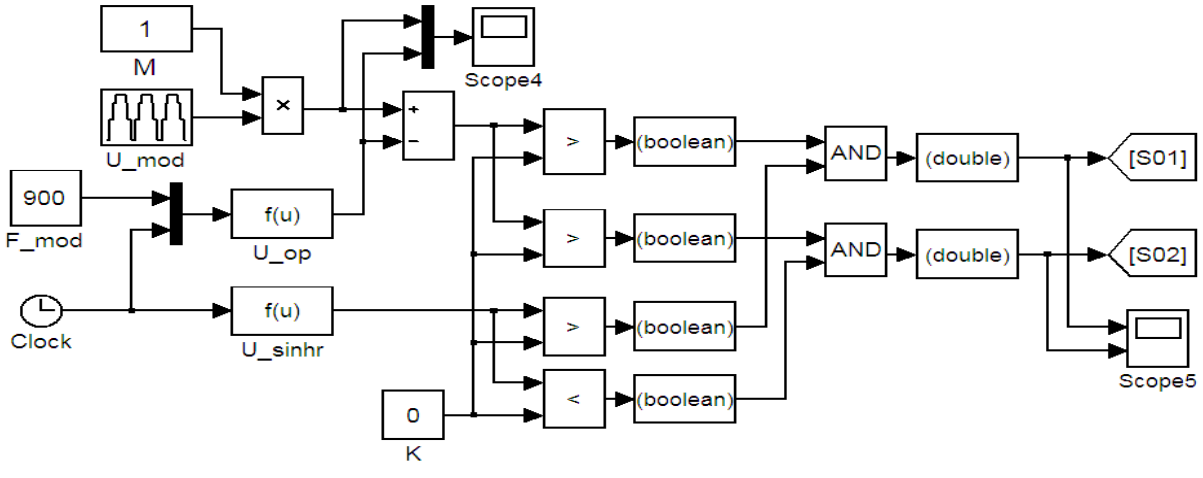

b

Fig. 4. Model of the active current-source rectifier in MATLAB: *a* — power part; *b* — control system

5. Results of the study of the active current-source rectifier with rectangular-stepped pulse-width modulation

It is known that the capacity of the ACSR input filter is selected on the basis of the permissible magnitude of the capacitor voltage fluctuations [18]. Probably, it is necessary to consider also that the reactive power consumption increases with increasing capacity.

With the help of the developed MATLAB model, the calculation of power factor for different capacity values in the nominal load mode (μ=1) was made. The capacitor capacity varied within 200...600 μF. As a result, the dependence of the power factor K_p on the input filter capacity C at a modulation frequency of 900, 1,200 and 1,800 Hz was obtained (Fig. 5). As can be seen from this dependence, the largest power factor is provided at C≈270...360 μF. For further calculations, the capacitor capacity was assumed to be C=360 μF at a frequency of 900 Hz and 1,200 Hz, C=300 μF at a frequency of 1,800 Hz.

Fig. 6 shows the wave forms of electromagnetic processes in the ACSR at f_m=1,200 Hz; μ=1. Since the discharge diode *VD*0 is used in the ACSR circuit, the rectified voltage waveform has the form of a sequence of positive polarity pulses. Voltage u_2 at the terminals of the secondary winding of the transformer has pulsations, the amplitude of which is limited by the capacity of the ACSR input filter capacitor. Current i_2 is non-sinusoidal and contains higher harmonics. Current i_v has a pulse form. Voltage u_1 at the terminals of the primary winding of the transformer is practically sinusoidal, and current i_1 is non-sinusoidal and has a close-to-zero phase shift relative to the voltage waveform u_1. The nature of electromagnetic processes at f_m=1,200 Hz; μ=0.6 (Fig. 7), in general, is similar.

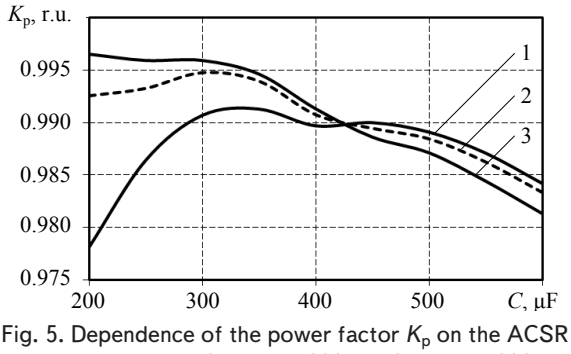

Fig. 5. Dependence of the power factor K_p on the ACSR input filter capacity C: 1 — f_m=900 Hz; 2 — f_m=1,200 Hz; 3 — f_m=1,800 Hz

Tables 2–4 present the results of computer simulation of the ACSR. The relative value of rectified voltage U_d/U_{d0} (U_{d0}=1,134 V is the nominal value of the average rectified voltage of the uncontrolled rectifier) does not exceed 0.84, and the ratio U_d/U_{d0} decreases with increasing PWM frequency. In order to obtain large values of U_d, it is necessary to transfer the ACSR to the over-modulation mode (μ>1) or to perform the secondary winding of the transformer for the larger nominal voltage U_2.

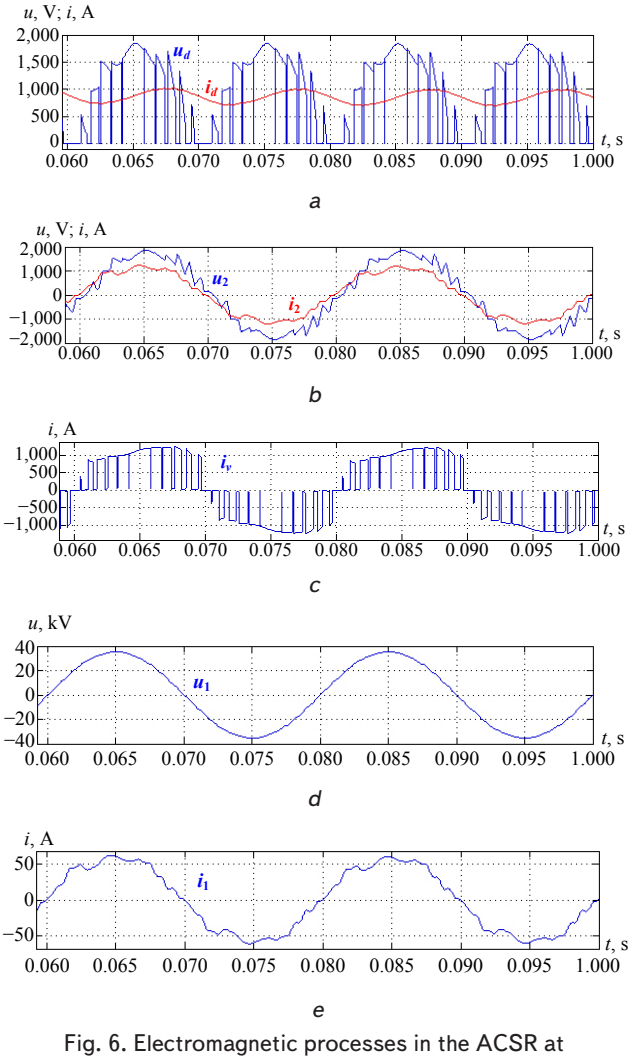

Fig. 6. Electromagnetic processes in the ACSR at f_m=1,200 Hz; μ=1: *a* – rectified voltage ud and current i_d; *b* – voltage u_2 and current i_2 of the secondary winding of the transformer; *c* – ACSR input current i_v; *d* – voltage of the primary winding of the transformer u_1; *e* – current of the primary winding of the transformer i_1

According to Tables 2–4, the average power factor was: K_{ap}=0.879 (900 Hz), K_{ap}=0.884 (1,200 Hz), K_{ap}=0.932 (1,800 Hz).

Table 2

Results of the ACSR simulation (f_m=900 Hz, C=360 μF)

v, km/h	μ	U_d, V	K_p	K_U, %	K_I, %	U_d/U_{d0}
30	0.2	195	0.623	0.43	11.82	0.17
35	0.4	389	0.857	1.03	21.36	0.34
40	0.6	581	0.941	1.60	23.39	0.51
45	0.8	767	0.984	1.68	14.48	0.68
50	1.0	950	0.991	1.74	13.19	0.84

Based on the results of the experiments, the dependences of total voltage (Fig. 8) and current (Fig. 9) harmonic distortion of the primary winding of the transformer on the modulation index are constructed.

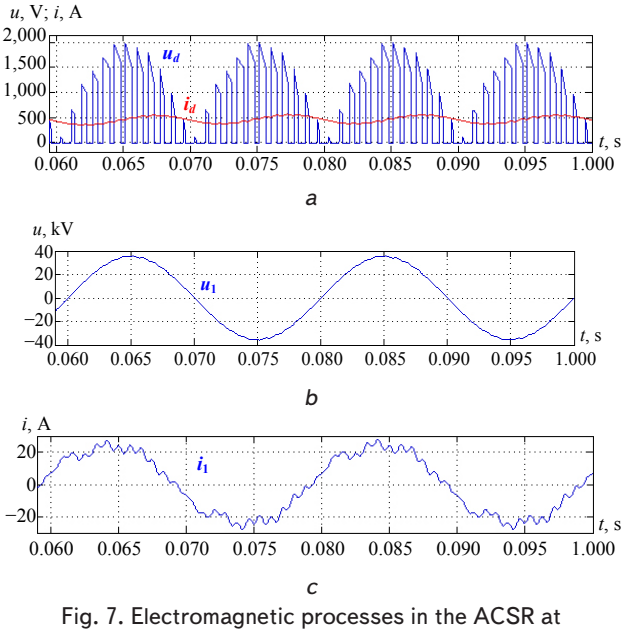

Fig. 7. Electromagnetic processes in the ACSR at f_m=1,200 Hz; μ=0.6: *a* – rectified voltage u_d and current i_d; *b* – voltage of the primary winding of the transformer u_1; *c* – current of the primary winding of the transformer i_1

Table 3

Results of the ACSR simulation (f_m=1,200 Hz, C=360 μF)

v, km/h	μ	U_d, V	K_p	K_U, %	K_I, %	U_d/U_{d0}
30	0.2	192	0.622	0.29	6.50	0.17
35	0.4	383	0.864	0.68	11.97	0.34
40	0.6	573	0.955	1.04	14.05	0.51
45	0.8	759	0.987	1.15	10.37	0.67
50	1.0	941	0.993	1.28	10.75	0.83

Table 4

Results of the ACSR simulation (f_m=1,800 Hz, C=360 μF)

v, km/h	μ	U_d, V	K_p	K_U, %	K_I, %	U_d/U_{d0}
30	0.2	187	0.793	0.22	5.09	0.16
35	0.4	374	0.908	0.49	7.93	0.33
40	0.6	560	0.973	0.74	9.12	0.49
45	0.8	743	0.992	0.84	8.44	0.66
50	1.0	924	0.996	0.93	8.55	0.81

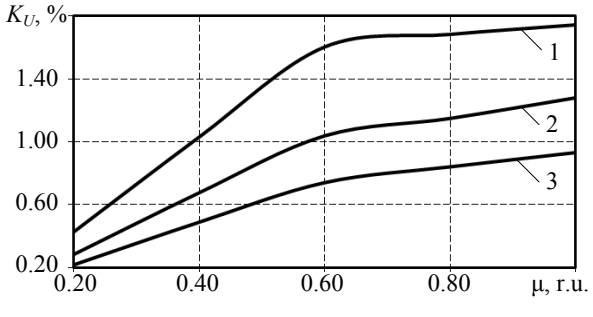

Fig. 8. Dependence of the total harmonic voltage distortion K_U of the primary winding of the transformer on the modulation index μ: 1 – f_m=900 Hz; 2 – f_m=1,200 Hz; 3 – f_m=1,800 Hz

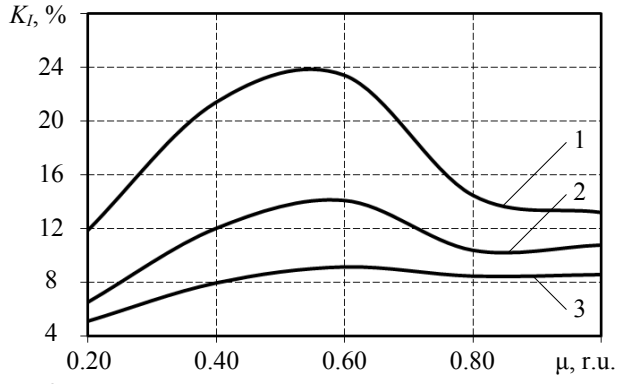

Fig. 9. Dependence of the total harmonic current distortion K_I of the primary winding of the transformer on the modulation index μ: 1 – f_m=900 Hz; 2 – f_m=1,200 Hz; 3 – f_m=1,800 Hz

6. Discussion of the results of the study of the active current-source rectifier

As can be seen from Tables 2–4, the power factor of the ACSR for all selected PWM frequencies is 0.62...0.99, and the value of more than 0.9 is provided with the modulation index of μ≥0.5. It should be noted that as the modulation frequency increases, the power factor increases over the entire load range, while compensation of inactive power components requires the smaller input filter capacity C.

In the paper, only a preliminary selection of the capacitor capacity C was made. The development of a technique for determining the ACSR input filter parameters, taking into account two criteria – the magnitude of the capacitor voltage fluctuations and reactive power consumption – is beyond the scope of the paper and is the subject of further research.

The total harmonic voltage distortion K_U in all considered cases does not exceed 2 %, and at a PWM frequency of 1,800 Hz – no more than 1 %; it increases with increasing modulation index and decreases with increasing PWM frequency.

The nature of changes in the total harmonic current distortion K_I is different: it reaches the maximum value in the modes where the pulse and pause intervals are approximately equal, i. e., for μ≈0.5...0.6. As the PWM frequency increases, there is a significant reduction in the total harmonic current distortion: if the maximum value of K_I at a frequency of 900 Hz is 23.39 %, then at a frequency of 1,800 Hz it is 9.12 %. According to this indicator, the ACSR with a modulation frequency of 900 Hz doesn't virtually differ from the traction thyristor converter, for which KI is about 20...30 % with the rectangular current waveform [21]. However, the current waveform distortion in the thyristor converter is determined mainly by low-frequency harmonics (3rd, 5th, 7th), while in the ACSR the greatest influence on such distortion is exerted by high-frequency harmonics with frequencies close to the PWM frequency (see the current waveform i1 in Fig. 6, *e*). Given that the considered ACSR operates as a DC regulator, and not as an active filter, the problem of compensation of higher harmonics of the input current requires a separate consideration.

Thus, in the ACSR, the PWM algorithm affects the current waveform to a greater extent. Therefore, when developing automatic control systems for rectifiers of this class, devices should be provided that ensure the input current waveform correction.

The results of the experiments allow concluding that, according to the set of selected comparison criteria, the ACSR with a modulation frequency of 1,200 Hz is considered the most suitable for implementation in the traction electric drive of the electric locomotive. It seems promising to develop a multi-zone converter on the basis of the ACSR and to study its operation in the traction electric drive of the AC electric locomotive with collector traction motors.

7. Conclusions

1. The mathematical model of the active current-source rectifier for the case of single-phase bridge circuit with a discharge diode and load in the form of DC traction motor is developed. The main ratios for pulse-width modulation with the unipolar rectangular-stepped modulating signal are determined. To solve the differential and logical equations describing the operation of the ACSR power part and control system, the MATLAB model is developed.

2. Electromagnetic processes in the rectification mode at three PWM frequencies (900, 1,200, 1,800 Hz) are studied. It is found that when the modulation index is varied within 0.2...1, the power factor of the ACSR is 0.6...0.99 regardless of the modulation frequency.

3. With pulse-width modulation in the active current-source rectifier, the total harmonic voltage distortion K_U in all cases does not exceed 2 %. The choice of a higher PWM frequency leads to an improvement of the AC waveform in the mains supply, but the use of voltage transformer is somewhat degraded.

4. According to the set of selected comparison criteria, the ACSR with a modulation frequency of 1,200 Hz is considered the most suitable for the implementation in the traction electric drive of the AC electric locomotive. The provision of high power characteristics in a wide range of traction loads can be achieved in the multi-zone circuit of such a converter, which should be taken into account in further research.

References

1. Quality assessment of control over the traction valve-inductor drive of a hybrid diesel locomotive / Buriakovskyi S., Babaiev M., Liubarskyi B., Maslii A., Karpenko N., Pomazan D. et. al. // Eastern-European Journal of Enterprise Technologies. 2018. Vol. 1, Issue 2 (91). P. 68–75. doi: 10.15587/1729-4061.2018.122422
2. Yeritsyan B., Liubarskyi B., Iakunin D. Simulation of combined body tilt system of high-speed railway rolling stock // Eastern-European Journal of Enterprise Technologies. 2016. Vol. 2, Issue 9 (80). P. 4–17. doi: 10.15587/1729-4061.2016.66782
3. Optimization of thermal modes and cooling systems of the induction traction engines of trams / Liubarskyi B., Petrenko O., Iakunin D., Dubinina O. // Eastern-European Journal of Enterprise Technologies. 2017. Vol. 3, Issue 9 (87). P. 59–67. doi: 10.15587/1729-4061.2017.102236

4. Analysis of optimal operating modes of the induction traction drives for establishing a control algorithm over a semiconductor transducer / Liubarskyi B., Petrenko A., Shaida V., Maslii A. // Eastern-European Journal of Enterprise Technologies. 2017. Vol. 4, Issue 8 (88). P. 65–72. doi: 10.15587/1729-4061.2017.109179
5. Shreyner R. T. Matematicheskoe modelirovanie elektroprivodov peremennogo toka s poluprovodnikovymi preobrazovatelyami chastoty. Ekaterinburg: URO RAN, 2000. 654 p.
6. Pou J., Wu B. High Power Converters: Topologies, Controls and Applications: Tutorial // IEEE IECON. France, 2006.
7. Zak V. V., Zarif'yan A. A., Kolpahch'yan P. G. Uluchshenie energeticheskih pokazateley elektrovozov peremennogo toka s zonno-faznym regulirovaniem napryazheniya // Visnyk Skhidnoukrainskoho natsionalnoho universytetu im. V. I. Dalia. 2011. Issue 4 (158). P. 185–190.
8. Michalík J., Molnár J., Peroutka Z. Single-Phase Current-Source Active Rectifier: Control Strategy under Distorted Power Supply Voltage // Przegląd Elektrotechniczny. 2009. Vol. 85, Issue 7. P. 148–453.
9. Yagovkin D. A. Razrabotka matematicheskoy modeli vypryamitel'no-invertornogo preobrazovatelya na IGBT-tranzistorah dlya elektrovoza peremennogo toka i ego bloka upravleniya v rezhime tyagi // Sovremennye tekhnologii. Sistemniy analiz. Modelirovanie. 2015. Issue 3 (47). P. 197–202.
10. Michalík J., Molnár J., Peroutka Z. Active Elimination of Low-Frequency Harmonics of Traction Current-Source Active Rectifier // Transactions on Electrical Engineering. 2012. Vol. 1, Issue 1. P. 30–35.
11. Michalik J., Molnar J., Peroutka Z. Behavior of active current source rectifier under critical transient conditions in traction // 2012 15th International Power Electronics and Motion Control Conference (EPE/PEMC). 2012. doi: 10.1109/epepemc.2012.6397245
12. Michalík J., Molnár J., Peroutka Z. Single Phase Current-Source Active Rectifier for Traction: Control System Design and Practical Problems // Advances in Electrical and Electronic Engineering. 2011. P. 86–89.
13. Chaudhary P., Samanta S., Sensarma P. Input-Series–Output-Parallel-Connected Buck Rectifiers for High-Voltage Applications // IEEE Transactions on Industrial Electronics. 2015. Vol. 62, Issue 1. P. 193–202. doi: 10.1109/tie.2014.2327556
14. Liu Y., Su M., Sun Y. Active power compensation method for single-phase current source rectifier without extra active switches // IET Power Electronics. 2016. Vol. 9, Issue 8. P. 1719–1726. doi: 10.1049/iet-pel.2015.0899
15. Efimov A. A., Mel'nikov S. Yu. Regulirovochnye harakteristiki aktivnyh odnofaznyh preobrazovateley toka // Zavalishinskie chteniya. Sankt-Peterburg: GUAP, 2016. P. 114–119.
16. Chaplygin E. E. Invertory napryazheniya i ih spektral'nye modeli: ucheb. pos. Moscow: Izdatel'stvo MEI, 2003. 64 p.
17. Get'man G. K. Teoriya elektricheskoy tyagi. Vol. 1: monografiya. Dnepropetrovsk: Izd-vo Makoveckiy, 2011. 456 p.
18. Elektronika i mikroskhemotekhnika. Vol. 4. Kn. 1. Sylova elektronika: navch. pos. / Senko V. I. et. al.; V. I. Senko (Ed.). Kyiv: Karavela, 2012. 640 p.
19. Strizhnev A. G., Lednik G. V. Sintez napryazheniy mnogokratnyh ravnomernyh ShIM, sozdannyh po stupenchatym funkciyam postroeniya // Energetika. Izvestiya vysshih uchebnyh zavedeniy i energeticheskih ob'edineniy SNG. 2011. Issue 5. P. 24–30.
20. Shavelkin A. A. Aktivniy vypryamitel' toka dlya preobrazovateley chastoty na baze avtonomnogo invertora toka // Nauchniy vestnik DGMA. 2012. Issue 2 (10E). P. 139–147.
21. Kulinich Yu. M. Adaptivnaya sistema avtomaticheskogo upravleniya gibridnogo kompensatora reaktivnoy moshchnosti elektrovoza s plavnym regulirovaniem napryazheniya: monografiya. Habarovsk: DVGUPS, 2001. 153 p.